Korean J. Chem. Eng., **29**(10), 1418-1425 (2012)
DOI: 10.1007/s11814-012-0052-x

Measurement and correlation of the isothermal vapor-liquid equilibrium data for carbon dioxide and dimethyl ether system

Min Hee Lee, Joon-Hyuk Yim, and Jong Sung Lim†

Department of Chemical and Biomolecular Engineering, Sogang University, Seoul 100-611, Korea

(*Received 18 January 2012 • accepted 17 April 2012*)

Abstract−Vapor-liquid equilibrium (VLE) data for the binary system of carbon dioxide (CO_2)+dimethyl ether (DME) were measured at six equally spaced (10 K) temperatures between 283.15 and 333.15 K. The data in the two-phase region were measured by using a circulation-type equilibrium apparatus in which both vapor and liquid phases are continuously recirculated. The equilibrium compositions of vapor and liquid phases and pressure were reported at each temperature. The experimental VLE data were correlated with PR-EoS using the Wong-Sandler (W-S) mixing rule and the universal mixing rule (UMR). The overall average values of AAD-P (%) and AAD-y through the temperature range from 283.15 to 333.15 K were 1.0% and 0.012 for the W-S mixing rule and 0.88% and 0.014 for the UMR, respectively. All values are small and acceptable. Calculated results with these equations have given satisfactory results compared with the experimental data.

Key words: Vapor-liquid Equilibrium, Carbon Dioxide, Dimethyl Ether, Peng-Robinson Equation of State, Wong-Sandler Mixing Rule

INTRODUCTION

Dimethyl carbonate (DMC) is considered as an alternative of methyl tert-butyl ether (MTBE), additive for non-leaded gasoline with its fast biodegradation rate and low toxicity [1]. Furthermore, DMC is a green alternative for corrosive and toxic dimethyl sulfate, methyl halide, and phosgene in methylation and carbonylation reactions [2,3]. It is nontoxic to humans and the environment [2]. And supercritical carbon dioxide ($scCO_2$) is among the most attractive green alternatives to replace conventional reagents and solvents employed in separation and reaction processes [4].

Many research groups are studying the direct synthesis of DMC starting from methanol and $scCO_2$ and the associated industrial manufacturing process [5,6]. This method is environmentally attractive because it uses only $scCO_2$ and methanol as raw materials and produces DMC and water, unlike other synthesis methods that use or produce toxic chemicals. DME and methyl iodide are byproducts of direct DMC synthesis [7].

Because this direct synthesis system involves carbon dioxide (CO_2) and dimethyl ether (DME) or other reaction products (DMC, water, CH_3I) at different temperature and pressure, vapor-liquid equilibrium (VLE) data is essential for evaluating the performance of DMC synthesis processes, determining their optimal composition, and designing the optimum separation process. For all these reasons, its thermodynamic properties were recently studied. However, there are few experimental data reported in the literature for CO_2+DME (CH_3OCH_3) system [8-10].

In this work, isothermal VLE data for binary mixture of CO_2+DME at six equally spaced temperatures from 283.15 to 333.15 K were measured by using a circulation-type equilibrium apparatus in which both phases were continuously recirculated. The experimental data were correlated with the PR-EoS [11] using the Wong-Sandler (W-S) mixing rule [12] and the universal mixing rule (UMR) [13,14]. In the range of experimental temperature, the average absolute deviations of pressure and vapor phase compositions between experimental and calculated values were determined and the relevant parameters were presented.

EXPERIMENTAL SECTION

1. Chemicals

High-grade chemicals of CO_2 and DME were used for VLE measurement. The CO_2 was purchased from Deok Yang Energen (Korea) (greater than 99 mass %), and the DME was purchased from Sigma Aldrich (USA) (greater than 99 mass %). We also analyzed these two pure components with a gas chromatograph. The resulting mass fraction purities of CO_2 and DME were greater than 99.5 mass %, so they were used without any further purification.

2. Experimental Apparatus

Although the vapor-liquid equilibrium apparatus used in this work is the same as that used in previous work [15-20], it is only briefly described here (Fig. 1). It was a circulation-type in which both liquid and vapor phases were recirculated continuously. The equilibrium cell is a type-316 stainless steel vessel within an inner volume of about 85 cm^3. In its middle part, two Pyrex glass windows of 20 mm thickness are installed front and back so that the liquid level, mixing and circulating behaviors, and critical phenomena can be observed by a back light during operation. A stirrer, rotated at variable speeds by an external magnet, was used to accelerate the attainment of the equilibrium state and to reduce concentration gradients in both phases.

The temperature of the equilibrium cell in the water bath was

---

†To whom correspondence should be addressed.
E-mail: limjs@sogang.ac.kr

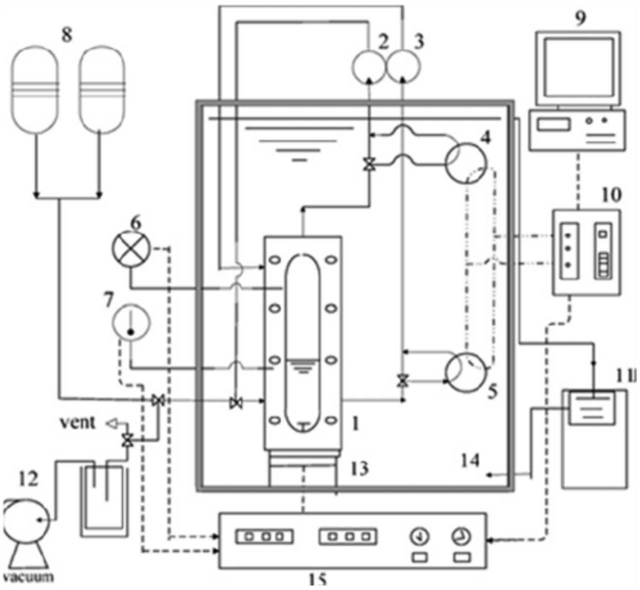

Fig. 1. Schematic diagram of the experimental apparatus.

1. Equilibrium cell
2. Vapor circulation pump
3. Liquid circulation pump
4. Liquid sample valve
5. Vapor sample valve
6. Temperature indicator
7. Pressure indicator
8. Sample reservoir
9. Computer
10. Gas chromatograph
11. Circulator
12. Vacuum pump
13. Magnetic stirrer
14. Constant temperature water bath
15. Display and controller

maintained by a circulator from Thermo Fisher Scientific, USA. The temperature in the cell was measured with a platinum-resistance sensor and a digital temperature indicator model F250MkII precision thermometer from Automatic Systems Laboratories, Ltd., United Kingdom. They were calibrated by the National Measurement Accreditation Service accredited calibration laboratory. The total uncertainty in temperature measurements is estimated to be within 0.01 K, including sensor uncertainty, temperature resolution, 0.001 K, and measurement uncertainty, 0.001 K. The pressure was measured with a pressure transducer, Model XPM60, and a digital pressure calibrator, Model PC106, from Beamax, Finland. Pressure calibrations are traceable to National Standards (Center for Metrology and Accreditation Cert. No. M-95P077, 14.11.1995, M-M 730, 16.11.1995, and M-95P078, 16.11.1995), the calibrator uncertainty was 0.0005 MPa, the pressure transducer uncertainty was 0.001 MPa, and the pressure indicator uncertainty was 0.001 MPa. Therefore, the total uncertainty of the pressure measurement is estimated to be within 0.001 MPa.

The vapor and liquid phases in the equilibrium cell were continuously recirculated by a dual-head circulation pump from the Milton Roy Company in order to reach the equilibrium state rapidly in the cell. The composition of the phases was determined by means of a gas chromatograph of Gow-Mac model 550P connected online to the VLE cell. The response of the thermal-conductivity detector (TCD) was carefully calibrated using the mixture prepared gravimetrically and the gas chromatographers (GC) with a Porapak Q column (length: 160 mm, I.D.: 1.5 mm, O.D.: 3.2 mm) from Alltech Company. We used helium gas (He) as a carrier gas and the flow rate was 30 ml/min. The temperature conditions of injector, oven and detector were 453.15, 433.15 and 453.15 K, respectively. Data derived from gas chromatography were treated with a computer program (Autochro-WIN from Young-Lin Instrument Co., Ltd.).

3. Experimental Procedure

To measure VLE data for the binary system of CO_2+DME, the system was first evacuated to remove all inert gases. A certain amount of DME was supplied to the cell, and then the temperature of the entire system was held constant by controlling the temperature of the water bath. After the desired temperature was attained, the pressure of the pure component was measured. A certain amount of CO_2 was introduced into the cell from a sample reservoir. Both the vapor and liquid phases were recirculated by a dual-head circulation pump until an equilibrium state was established. Two hours were sufficient to obtain thermal equilibrium between the cell fluid and the thermostatic bath as well as between the vapor and liquid phases. After equilibration was reached, the pressure in the equilibrium cell was measured, and then vapor and liquid samples were withdrawn from the recycling lines by the vapor and liquid sampling valves, respectively. The compositions of the samples were measured by immediately injecting them into the GC, which was connected online to the vapor and liquid sampling valves. The GC was calibrated with pure components of known purity and with mixtures of known composition that were prepared gravimetrically. At least five analyses were performed for each phase, and the average values were considered to correspond to the equilibrium values. Considering the margin of error and the reproducibility of the GC, we estimated an overall uncertainty of 0.002 in the measurements of the mole fraction for both the liquid and the vapor phases.

CORRELATION

1. Correlation with the PR- EoS Using the W-S Mixing Rule

The experimental VLE data were correlated with the PR-EoS [11] using the W-S mixing rule [12]. The PR EoS and the W-S mixing rules are expressed as follows:

$$P=\frac{RT}{v-b}-\frac{a(T)}{v(v+b)+b(v-b)} \tag{1}$$

with

$$a(T)=\left(0.457235\frac{R^2T_c^2}{P_c}\right)\alpha(T) \tag{2}$$

$$b=0.077796\frac{RT_c}{P_c} \tag{3}$$

$$\alpha(T)=[1+k(1-\sqrt{T/T_c})]^2 \tag{4}$$

$$k=0.37464+1.54226\omega-0.26992\omega^2 \tag{5}$$

where the parameter a is a function of temperature, b is constant, k is a constant characteristic of each substance, ω is the acentric factor, P is the pressure, P_c is the critical pressure, T is the absolute temperature, T_c is the critical temperature, and v is the molar volume of the mixture.

The W-S mixing rules [12] were used in this work to obtain EoS parameters for a mixture from those of the pure components. These mixing rules for a cubic equation of state can be written as

$$b_m = \frac{\sum_i \sum_j x_i x_j (b - a/RT)_{ij}}{\left(1 - A^E_\infty / CRT - \sum_i x_i a_i / RTb_i\right)} \tag{6}$$

with

$$(b - a/RT)_{ij} = \frac{1}{2}[(b - a/RT)_i + (b - a/RT)_j](1 - k_{ij}) \tag{7}$$

and

$$\frac{a_m}{b_m} = \sum_i x_i \frac{a_i}{b_i} + \frac{A^E_\infty}{C} \tag{8}$$

where C is a numerical constant equal to $\ln(\sqrt{2} - 1)/\sqrt{2}$ for the PR-EoS used in this work. The single adjustable parameter (k_{ij}) for each binary pair is referred to as the W-S mixing rule parameter. Also, A^E_∞ is an excess Helmholtz free energy model at infinite pressure that can be equated to a low-pressure excess Gibbs energy model [21]. In this study, we used the nonrandom two-liquid (NRTL) model [22] given by

$$\frac{A^E_\infty}{RT} = \sum_i x_i \frac{\sum_j x_j G_{ji} \tau_{ji}}{\sum_r x_r G_{ri}} \tag{9}$$

with

$$G_{ji} = \exp(-\alpha_{ji}\tau_{ji}) \text{ and } \tau_{ji} = (g_{ji} - g_{ii})/(RT) \tag{10}$$

The critical temperature (T_c), critical pressure (P_c), and acentric factor (ω) for both CO_2 and DME, which were used to calculate the parameters for the PR-EoS, are provided in Table 1. We have set the non-randomness parameter, α_{ij} equal to a fixed value of 0.3 in this study. The parameters of the PR-EoS were obtained by minimizing the following objective function:

$$\text{objective function} = \frac{1}{N}\sum_j^N \left[\left(\frac{P_{j,exp} - P_{j,cal}}{P_{j,exp}}\right) \times 100\right]^2 \tag{11}$$

2. Correlation with the PR-EoS Using the UMR

The experimental VLE data were also correlated with the PR-EoS, the Mathias-Copeman function [23], and the UMR suggested by Voutsas et al. [13,14]. The UMR mixing rule can be expressed as:

$$a = \frac{1}{A}\frac{G^{E,SG}_{AC} + G^{E,res}_{AC}}{RT} + \sum_i x_i a_i \tag{12}$$

A in Eq. (12) is a constant that depends on the cubic EoS used. And the Mathias-Copeman function is defined as:

$$\alpha(T) = [1 + c_1(1 - \sqrt{T_r}) + c_2(1 - \sqrt{T_r})^2 + c_3(1 - \sqrt{T_r})^3]^2 \tag{13}$$

The parameters c_i are derived with vapor pressures for the pure components. The parameter b is also calculated with properties of the pure components.

$$b = \sum_i \sum_j x_i x_j b_{ij};\quad b_{ij} = \left(\frac{b_i^{1/2} + b_j^{1/2}}{2}\right)^2 \tag{14}$$

Table 1. Thermodynamic properties of components

Chemical	Chemical formula	T_c/K	P_c/MPa	ω
Carbon dioxide [27]	CO_2	304.21	7.384	0.2239
Dimethyl ether [29]	CH_3OCH_3	400.10	5.4398	0.2002

The terms $G^{E,SG}_{AC}$ and $G^{E,res}_{AC}$ represent, respectively, the Staverman-Guggenheim term and residual term in the UNIQUAC [24] or UNIFAC [25] activity-coefficient (AC) model. The Staverman-Guggenheim contribution is given as:

$$G^{E,SG}_{AC}/RT = \frac{z}{2}\left(q_1 x_1 \ln\frac{\Phi_1}{x_1} + q_2 x_2 \ln\frac{\Phi_2}{x_2}\right) \tag{15}$$

with

$$\Phi_1 = \frac{x_1 r_1}{x_1 r_1 + x_2 r_2},\quad \Phi_2 = \frac{x_2 r_2}{x_1 r_1 + x_2 r_2} \tag{16}$$

And the residual contribution is

$$G^{E,res}_{AC}/RT = -q_1 x_1 \ln(\theta_1 + \theta_2 \tau_{21}) - q_2 x_2 \ln(\theta_2 + \theta_1 \tau_{12}) \tag{17}$$

with

$$\theta_1 = \frac{x_1 q_1}{x_1 q_1 + x_2 q_2},\quad \theta_2 = \frac{x_2 q_2}{x_1 q_1 + x_2 q_2} \tag{18}$$

and

$$\tau_{12} = \exp(-\varepsilon_{12}/RT),\quad \tau_{21} = \exp(-\varepsilon_{21}/RT) \tag{19}$$

Volume parameters (r_1 and r_2) and surface area parameters (q_1 and q_2) are required as pure-component properties and are calculated with the method of Bondi [26]. Note that the Flory-Huggins terms in the activity-coefficient expressions are removed due to overlap with the cubic EoS terms, as indicated by Voutsas et al. [13,14]. For a given T-p-x-y dataset at isothermal condition, two binary interaction parameters (ε_{12} and ε_{21} in Eq. (19)) are fitted, and bubble-pressure calculation results are compared with the experimental data.

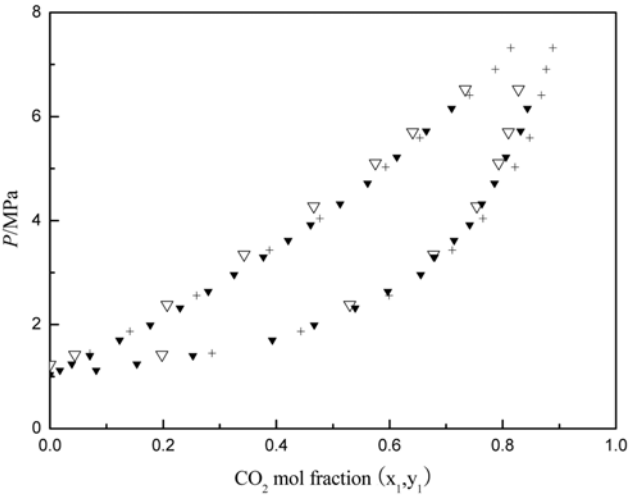

Fig. 2. Comparison of our experimental data with literature data for the CO_2 (1)+DME (2) system. Experimental data of this work: ▽, T=323.15 K, our work; ▼, 320.12 K, Jónasson et al. [9]; +, 320.15 K, Laursen et al. [10].

Table 2. Comparison of the measured pure component vapor pressures

Component	T/K	P_{exp}/MPa	P_{ref}/MPa	ΔP/MPa	$\lvert\Delta P\rvert/P_{exp}$/%
Carbon dioxide (1)	283.15	4.495	4.497[a]	−0.002	0.044
	293.15	5.742	5.772[a]	−0.030	0.522
	303.15	7.218	7.205[a]	0.013	0.180
					Ave 0.25
Dimethyl ether (2)	283.15	0.374	0.386[b]	−0.012	3.201
	293.15	0.531	0.532[b]	−0.001	0.188
	303.15	0.717	0.718[b]	−0.001	0.140
	313.15	0.945	0.949[b]	−0.004	0.423
	323.15	1.227	1.231[b]	−0.004	0.326
	333.15	1.565	1.571[b]	−0.006	0.383
					Ave 0.78

[a] Data can be obtained from the literature [27]
[b] Data can be obtained from the literature [28]

RESULTS AND DISCUSSION

The equilibrium compositions for the CO_2 (1)+DME (2) binary systems were measured at six equally spaced temperatures from (283.15 to 333.15) K. To verify the consistency of our experimental data, we compared our experimental data at 323.15 K with literature data already reported by Jónasson et al. [9] and Laursen et al. [10] at similar temperatures 320.12 K, 320.15 K, respectively in Fig. 2. As can be seen from Fig. 2, although an exact comparison could not be made because of the temperature differences, the tendency of our experimental data agreed well with the literature data reported by Jónasson et al. [9] and Laursen et al. [10].

In Table 2 the comparison between the measured vapor pressure of pure CO_2 and DME is presented. The pure component data is considered to be reliable and consistent with available literature data. The average of the relative deviation ($\sum|\Delta P/P|/N$ (%)) between the measured and calculated value was 0.25% for CO_2 from the database REFPROP 6.01 [27] and 0.78% for DME from the Poling-Prausnitz-O'Connell book [28], respectively. The experimental VLE data and the results of the correlation are reported in Table 3. This table lists the

Table 3. Vapor-liquid equilibrium measurements for the CO_2 (1)+DME (2) system

Experimental data			PR EOS(W-S)/NRTL				PR EOS(UMR)/UNIQUAC			
P_{exp}/MPa	$x_{1,exp}$	$y_{1,exp}$	P_{cal}/MPa	$y_{1,cal}$	[a]ΔP/Mpa	[b]Δy_1	P_{cal}/MPa	$y_{1,cal}$	[a]ΔP/Mpa	[b]Δy_1
					283.15 K					
0.374	0.000	0.000	0.379	0.000	−0.005	0.000	0.374	0.000	0.000	0.000
0.533	0.065	0.275	0.533	0.316	0.000	−0.041	0.532	0.320	0.002	−0.045
0.862	0.185	0.608	0.857	0.608	0.005	0.000	0.862	0.612	0.000	−0.004
1.470	0.371	0.777	1.465	0.806	0.005	−0.029	1.474	0.806	−0.004	−0.029
2.284	0.573	0.890	2.278	0.904	0.006	−0.015	2.275	0.902	0.009	−0.013
3.071	0.744	0.937	3.077	0.951	−0.006	−0.014	3.062	0.949	0.009	−0.012
3.633	0.854	0.961	3.643	0.973	−0.010	−0.011	3.626	0.972	0.007	−0.010
4.079	0.934	0.980	4.087	0.987	−0.008	−0.007	4.077	0.987	0.002	−0.007
4.495	1.000	1.000	4.503	1.000	−0.008	0.000	4.495	1.000	0.000	0.000
					293.15 K					
0.531	0.000	0.000	0.517	0.000	0.014	0.000	0.531	0.000	0.000	0.000
0.724	0.067	0.302	0.730	0.311	−0.006	−0.009	0.738	0.300	−0.014	0.001
0.965	0.135	0.473	0.965	0.496	0.000	−0.023	0.965	0.483	0.000	−0.010
1.607	0.301	0.701	1.607	0.727	0.000	−0.026	1.597	0.719	0.009	−0.018
2.413	0.482	0.832	2.435	0.846	−0.022	−0.014	2.415	0.842	−0.002	−0.010
2.965	0.588	0.877	2.979	0.889	−0.015	−0.012	2.959	0.886	0.006	−0.009
3.930	0.748	0.924	3.893	0.937	0.037	−0.012	3.878	0.935	0.052	−0.011
4.482	0.826	0.943	4.385	0.956	0.097	−0.012	4.379	0.955	0.103	−0.012
5.323	0.939	0.967	5.205	0.983	0.118	−0.016	5.200	0.982	0.123	−0.016
5.742	1.000	1.000	5.741	1.000	0.001	0.000	5.742	1.000	0.000	0.000

Table 3. Continued

Experimental data			PR EOS(W-S)/NRTL				PR EOS(UMR)/UNIQUAC			
P_{exp}/MPa	$x_{1,\,exp}$	$y_{1,\,exp}$	P_{cal}/MPa	$y_{1,\,cal}$	$^{a}\Delta P$/Mpa	$^{b}\Delta y_1$	P_{cal}/MPa	$y_{1,\,cal}$	$^{a}\Delta P$/Mpa	$^{b}\Delta y_1$
					303.15 K					
0.717	0.000	0.000	0.691	0.000	0.026	0.000	0.717	0.000	0.000	0.000
0.827	0.040	0.188	0.830	0.179	−0.002	0.009	0.850	0.169	−0.023	0.019
1.310	0.163	0.496	1.310	0.509	0.000	−0.012	1.316	0.493	−0.006	0.003
2.137	0.339	0.711	2.137	0.729	0.000	−0.017	2.134	0.720	0.004	−0.008
3.103	0.516	0.826	3.137	0.840	−0.035	−0.014	3.142	0.836	−0.040	−0.010
4.206	0.674	0.882	4.189	0.901	0.017	−0.019	4.206	0.899	0.000	−0.017
5.275	0.805	0.918	5.187	0.938	0.088	−0.021	5.222	0.937	0.053	−0.020
5.998	0.886	0.942	5.893	0.960	0.106	−0.018	5.938	0.959	0.061	−0.017
7.218	1.000	1.000	7.217	1.000	0.001	0.000	7.351	1.000	−0.134	0.000
					313.15 K					
0.945	0.000	0.000	0.906	0.000	0.039	0.000	0.945	0.000	0.000	0.000
1.241	0.075	0.294	1.249	0.287	−0.008	0.007	1.270	0.271	−0.029	0.023
1.834	0.191	0.524	1.834	0.532	0.000	−0.007	1.836	0.516	−0.002	0.008
2.758	0.353	0.717	2.758	0.709	0.000	0.009	2.758	0.701	0.000	0.016
3.723	0.492	0.798	3.667	0.797	0.056	0.000	3.681	0.795	0.042	0.003
4.630	0.624	0.848	4.652	0.856	−0.023	−0.008	4.680	0.855	−0.050	−0.007
5.836	0.769	0.882	5.897	0.904	−0.060	−0.022	5.939	0.904	−0.103	−0.022
6.353	0.811	0.895	6.304	0.917	0.049	−0.021	6.344	0.917	0.010	−0.021
					323.15 K					
1.227	0.000	0.000	1.167	0.000	0.060	0.000	1.227	0.000	0.000	0.000
1.420	0.044	0.198	1.428	0.183	−0.007	0.015	1.464	0.165	−0.044	0.033
2.379	0.207	0.530	2.430	0.528	−0.051	0.003	2.413	0.509	−0.034	0.021
3.344	0.343	0.678	3.344	0.665	0.000	0.013	3.306	0.656	0.037	0.022
4.275	0.466	0.754	4.242	0.745	0.032	0.010	4.212	0.743	0.063	0.012
5.102	0.575	0.793	5.119	0.797	−0.017	−0.004	5.108	0.799	−0.006	−0.006
5.701	0.641	0.810	5.701	0.823	0.000	−0.013	5.701	0.827	0.000	−0.017
6.526	0.734	0.828	6.581	0.854	−0.055	−0.027	6.609	0.860	−0.083	−0.032
					333.15 K					
1.565	0.000	0.000	1.481	0.000	0.084	0.000	1.565	0.000	0.000	0.000
1.758	0.046	0.167	1.789	0.169	−0.031	−0.002	1.844	0.152	−0.086	0.015
2.806	0.198	0.491	2.848	0.476	−0.042	0.015	2.842	0.458	−0.036	0.033
3.744	0.319	0.631	3.744	0.603	0.000	0.028	3.730	0.596	0.014	0.035
4.964	0.463	0.712	4.904	0.699	0.060	0.013	4.917	0.703	0.048	0.009
5.809	0.560	0.740	5.759	0.746	0.050	−0.006	5.809	0.754	0.000	−0.015
6.250	0.617	0.751	6.295	0.768	−0.045	−0.017	6.370	0.779	−0.120	−0.027
6.783	0.669	0.754	6.797	0.785	−0.014	−0.031	6.904	0.797	−0.121	−0.044

$^{a}\Delta P = P_{exp} - P_{cal}$

$^{b}\Delta y_1 = y_{exp} - y_{cal}$

Total uncertainty of the temperature is within 0.01 K

Total uncertainty of the pressure is within 0.001 MPa

Overall uncertainty of liquid and vapor phase mole fraction is within 0.002

measured mole fractions of the liquid and vapor phases, the pressures and temperatures in equilibrium and the deviations between measured and calculated pressures (ΔP) and vapor compositions (Δy).

Fig. 3 shows the comparison of measured and calculated values with the PR-EoS using the W-S mixing rule and PR-EoS using the UMR for the binary system of the CO_2+DME at various temperatures of 283.3, 293.15, 303.15, 313.15, 323.15 and 333.15 K. Also, the calculated values were well matched with experimental data. The interaction parameters of the binary mixtures for each isotherm, the binary parameters k_{ij}, and the absolute average deviations of pressure (AAD-P (%)) and the absolute average deviation of vapor-phase composition (AAD-y) between measured and calculated values for our work and the literature [8-10] are reported in Table 4. Fig. 4 plots the binary parameters, k_{ij}, vs. temperature. As can be seen in this figure and Table 4, the binary parameters k_{ij} show temperature dependency. They were fitted with 1st order polynomial equations

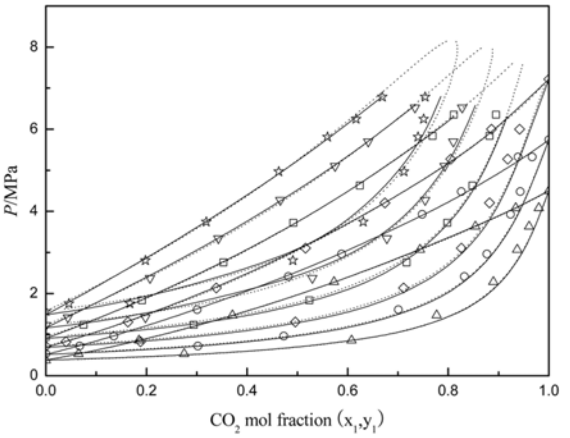

Fig. 3. P-x-y diagram for the system of CO_2 (1)+DME (2). Experimental data: △, T=283.15 K; ○, T=293.15 K; ◇, T=303.15 K; □, T=313.15 K; ▽, T=323.15 K; ☆, T=333.15 K. —, calculated with the PR EoS using W-S mixing rule; ---, calculated with the PR-EoS using UMR.

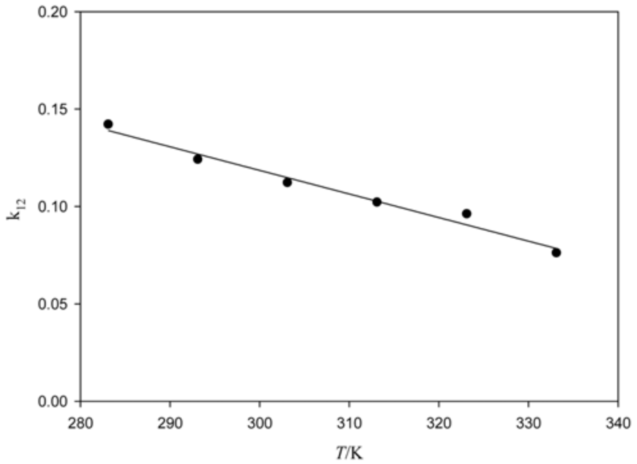

Fig. 4. Parameter k_{ij} obtained by using the PR-EoS with W-S mixing rule. The equation of the fitting line is k_{ij}=−0.0012 T/K+0.48 (333.15 K≥T≥283.15 K).

Table 4. Values of binary parameters and relative average deviations of P and y

Source of data	T/K	PR EOS(W-S)NRTL					PR EOS(UMR)/UNIQUAC			
		^{a}k$_{12}$	^{b}A$_{12}$	^{b}A$_{21}$	^{d}AAD-P (%)	^{e}AAD-y	^{c}A$_{12}$	^{c}A$_{21}$	^{d}AAD-P (%)	^{e}AAD-y
This work	283.15	0.14	48	−173	0.37	0.013	−1373	1349	0.17	0.013
	293.15	0.12	−38	−38	1.02	0.013	−1321	1318	0.87	0.009
	303.15	0.11	−80	−22	0.99	0.012	−1591	1583	0.94	0.010
	313.15	0.10	−303	349	1.07	0.009	−1421	1419	0.82	0.013
	323.15	0.10	−65	79	1.18	0.011	1337	−1340	1.06	0.018
	333.15	0.08	15	15	1.45	0.014	1448	−1452	1.40	0.022
	Overall				1.00	0.012			0.88	0.014
Lit. [8]	273.15	0.07	−48.57	−48.87	1.26	0.011	−2438	4578	0.45	0.017
	288.20	0.12	−58.41	−57.72	1.12	0.019	−1693	1574	0.28	0.021
	308.65	0.06	−27.04	−27.73	0.75	0.015	−630	223	0.36	0.020
	320.06	0.12	−33.84	−50.55	0.89	0.010	371	−700	0.53	0.010
	335.17	0.10	98.13	−119.66	1.07	0.012	−2301	3406	0.48	0.017
	350.20	0.08	880.89	−436.63	1.18	0.004	−990	964	0.48	0.012
	360.07	0.10	−50.03	50.36	1.84	0.006	−1006	1002	0.26	0.020
	370.13	0.14	−42.68	−34.83	1.63	0.007	−855	865	0.60	0.009
	377.57	0.09	−81.21	76.24	1.64	0.008	4259	−2553	0.28	0.007
	386.56	0.22	−284.40	138.45	2.27	0.002	−1131	1819	0.09	0.006
	Overall				1.40	0.009			0.38	0.014
Lit. [9]	288.20	0.13	203.44	−267.17	1.66	0.022	−257	−263	1.28	0.011
	308.65	0.10	−169.79	102.25	0.67	0.010	283	−631	0.37	0.012
	320.12	0.13	−16.84	−79.73	0.88	0.020	722	−915	0.44	0.023
	Overall				1.10	0.017			0.70	0.015
Lit. [10]	298.15	0.08	86.17	−76.34	0.29	0.005	286	−390	0.24	0.003
	308.65	0.14	104.81	−114.04	0.37	0.007	−694	694	0.32	0.007
	320.15	0.12	126.29	−144.15	1.22	0.006	−834	725	0.83	0.008
	Overall				0.63	0.006			0.46	0.006

^{a}k$_{12}$ is an interaction parameter

^{b}NRTL: $A_{12}=(g_{12}-g_{22})/R$, $A_{21}=(g_{21}-g_{22})/R$

^{c}UNIQUAC: $A_{12}=(u_{12}-u_{22})/R$, $A_{21}=(u_{21}-u_{22})/R$

^{d}AAD-P (%)$=(1/N)\Sigma|(P_{exp}-P_{cal})/P_{exp}|\times 100$

^{e}AAD-y$=(1/N)\Sigma|(y_{exp}-y_{cal})|$

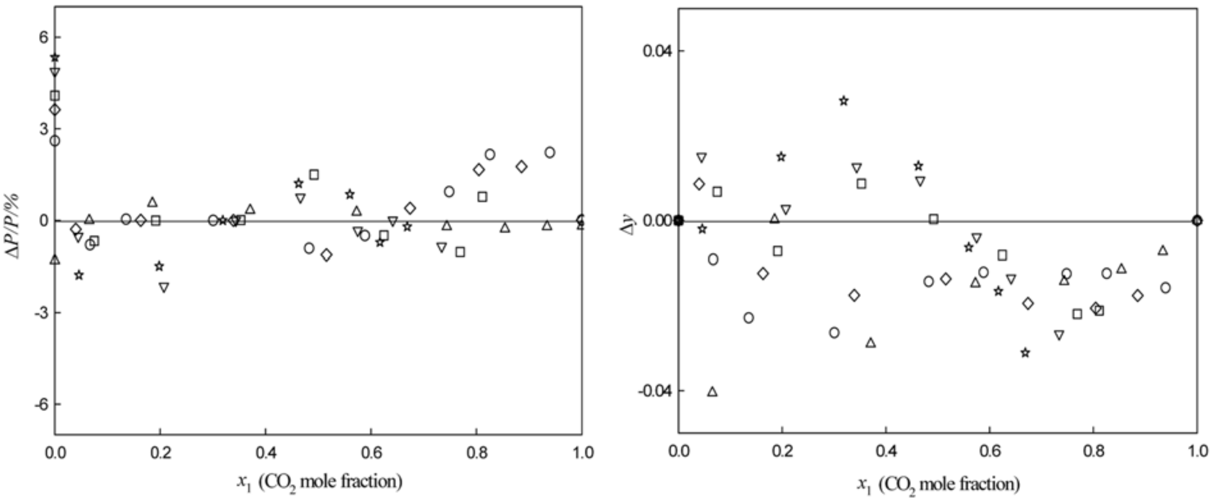

Fig. 5. Deviation of pressure and vapor composition for the system of CO_2 (1)+DME (2) from the PR- EoS using W-S mixing rule at: △, T=283.15 K; ○, T=293.15 K; ◇, T=303.15 K; □, T=313.15 K; ▽, T=323.15 K; ☆, T=333.15 K.

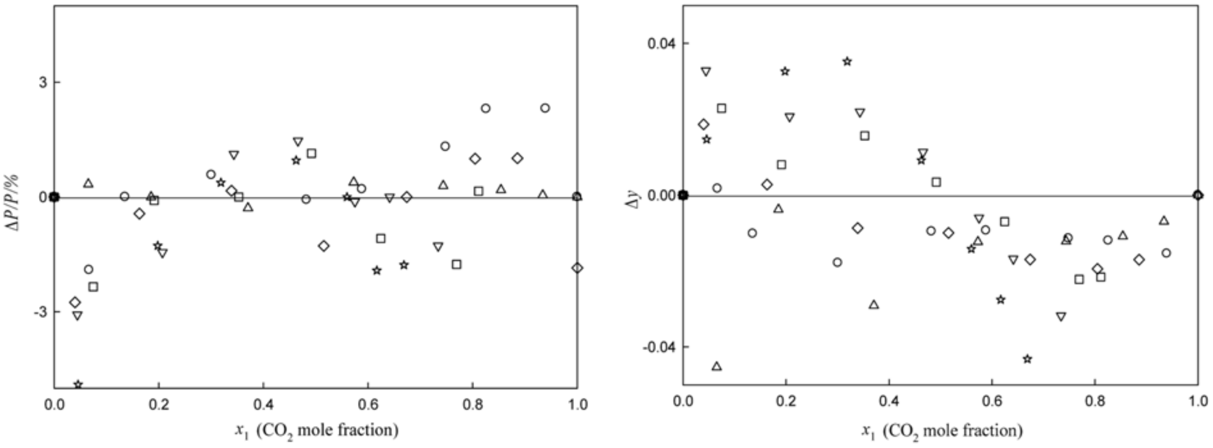

Fig. 6. Deviation of pressure and vapor composition for the system of CO_2 (1)+DME (2) from the PR- EoS using UMR at: △, T=283.15 K; ○, T=293.15 K; ◇, T=303.15 K; □, T=313.15 K; ▽, T=323.15 K; ☆, T=333.15 K.

for the temperature and k_{ij} is given by Eq. (20).

$$k_{ij}=-0.0012\ (T/K)+0.48 \qquad (20)$$

The overall average values of AAD-P (%) and AAD-y through the temperature range from 283.15 to 333.15 K were 1.0% and 0.012 for the PR-EoS using the W-S mixing rule and 0.88% and 0.014 for the PR-EoS using the UMR, respectively. All values are small and acceptable. In Figs. 5 and 6, the relative deviations of pressure ($\Delta P/P_{exp}$ %) and the vapor phase compositions (Δy_1) for the PR-EoS using the W-S mixing rule and the PR-EoS using the UMR were plotted with the liquid phase compositions (x_1), point by point. From these figures and the low average deviations of P and y, we conclude that the calculated values with the PR-EoS using the W-S mixing rules and the PR-EoS using the UMR give good agreements with the experimental data.

CONCLUSIONS

The isothermal VLE data for the binary systems of CO_2+dimethyl ether were measured in the temperature range from 283.15 to 333.15 K in 10 K intervals using a circulation-type equilibrium apparatus. The experimental VLE data were correlated with the PR-EoS using the W-S mixing rules and the UMR. The binary parameters k_{ij} show temperature dependency and were fitted with 1st order polynomial equations for the temperature as $k_{ij}=-0.0012$ (T/K)+0.48. The overall average values of AAD-P (%) and AAD-y through the temperature range from 283.15 to 333.15 K were 1.0% and 0.012 for the W-S mixing rule and 0.88% and 0.014 for the UMR, respectively. So, we conclude that the calculated values with the PR-EoS using both the W-S mixing rules and the UMR give good agreement with the experimental data.

ACKNOWLEDGEMENTS

This research was supported by Sogang University Research Grant in 2011.

NOMENCLATURE

a(T) : temperature dependent

a : attraction parameter
b : molecular volume
c : pure compound parameters as defined in Mathias-Copeman expression
P, P_c : pressure, critical pressure [MPa]
R : gas constant 8.3144 [$J\cdot mol^{-1}\ K^{-1}$]
k_{ij} : interaction Parameter
T, T_c : absolute temperature, critical temperature, reduced temperature [K]
v : molar volume
x : liquid mole fraction
y : vapor mole fraction
A_∞^E : excess Helmholtz free energy at infinite pressure
G, g : excess Gibbs energy [$J\cdot mol^{-1}$]

Greek Letters

ω : acentric factor
α : non-randomness parameter

Superscripts

res : residual term
SG : Staverman-Guggenheim contribution

Subscripts

AC : activity coefficient model
c : critical property
cal : calculated
exp : experimental
i, j : i th, j th component of the mixture
r : reduced property

REFERENCES

1. M. A. Pacheco and C. L. Marshall, *Energy Fuels*, **11**, 2 (1997).
2. Y. Ono, *Appl. Catal. A: Gen.*, **155**, 133 (1997).
3. P. Tundo and M. Selva, *Acc. Chem. Res.*, **35**, 706 (2002).
4. H. Matsuda, S. Yoshii, A. Nagashima, K. Kurihara and K. Ochi, *J. Chem. Eng. Data*, **50**, 1419 (2005).
5. S. Camy and J. S. Condoret, *Chem. Eng. Process.*, **40**, 499 (2001).
6. S. Camy, J. S. Pic, E. Badens and J. S. Condoret, *J. Supercrit. Fluids*, **25**, 19 (2003).
7. H. Matsuda, S. Yoshii, A. Nagashima, K. Kurihara and K. Ochi, *J. Chem. Eng. Data*, **50**, 1419 (2005).
8. C. Y. Tsang and W. B. Streett, *J. Chem. Eng. Data*, **26**, 155 (1981).
9. A. Jónasson, O. Persson and A. Fredenslund, *J. Chem. Eng. Data*, **40**, 296 (1995).
10. T. Laursen, P. Rasmussen and S. I. Andersen, *J. Chem. Eng. Data*, **47**, 198 (2002).
11. D. Y. Peng and D. B. Robinson, *Ind. Eng. Chem. Fundam.*, **15**, 59 (1976).
12. D. S. H. Wong and S. I. Sandler, *AIChE J.*, **38**, 671 (1992).
13. E. Voutsas, K. Magoulas and D. Tassios, *Ind. Eng. Chem. Res.*, **43**, 6238 (2004).
14. E. Voutsas, V. Louli, C. Boukouvalas, K. Magoulas and D. Tassios, *Fluid Phase Equilib.*, **241**, 216 (2006).
15. J. S. Lim, G. M. Seong and H. S. Byun, *Fluid Phase Equilib.*, **259**, 165 (2007).
16. J. S. Lim, G. M. Seong and H. K. Roh, *J. Chem. Eng. Data*, **52**, 1313 (2007).
17. J. S. Lim, G. Seong, H.-K. Roh and B. G. Lee, *J. Chem. Eng. Data*, **52**, 2250 (2007).
18. K. M. Seong, A. R. Kim, K. P. Yoo and J. S. Lim, *Korean J. Chem. Eng.*, **26**, 206 (2009).
19. J. W. Kang, A. R. Kim and J. S. Lim, *Korean J. Chem. Eng.*, **27**, 261 (2010).
20. S. A. Kim, K. P. Yoo and J. S. Lim, *Korean J. Chem. Eng.*, **27**, 1887 (2010).
21. D. S. H. Wong, H. Orbey and S. I. Sandler, *Ind. Eng. Chem. Res.*, **31**, 2033 (1992).
22. H. Renon and J. M. Prausnitz, *AIChE J.*, **14**, 135 (1968).
23. P. M. Mathias and T. W. Copeman, *Fluid Phase Equilib.*, **13**, 91 (1983).
24. T. F. Anderson, D. S. Abrams and E. A. Grens II, *AIChE J.*, **24**, 20 (1978).
25. A. Fredenslund, R. L. Jones and J. M. Prausnitz, *AIChE J.*, **21**, 1086 (1975).
26. A. A. Bondi, *Physical Properties of Molecular Crystals, Liquids, and Glasses*, John Wiley and Sons: Hoboken, New Jersey (1968).
27. M. O. McLinden, S. A. Klein, E. W. Lemmoon and A. P. Peskin, *Thermodynamic Properties of Refrigerants and Refrigerant Mixtures Database (REFPROP)*, V.6.01, NIST (1998).
28. B. E. Poling, J. M. Prasunitz and J. P. O'Connell, fifth Ed., McGraw-Hill, New York (2001).
29. J. Im, G. Lee, J. Lee and H. Kim, *J. Chem. Thermodyn.*, **38**, 1510 (2006).